Medicine & Science IN Sports & Exercise
The Official Journal of the American College of Sports Medicine
www.acsm-msse.org

. . . Published ahead of Print

Individual Region- and Muscle-specific Hamstring Activity at Different Running Speeds

András Hegyi[1], Basílio AM Gonçalves[1,2], Taija Finni[1], Neil J Cronin[1]

[1]Neuromuscular Research Center, Faculty of Sport and Health Sciences, University of Jyväskylä, Jyvaskyla, Finland; [2]School of Allied Health Sciences, Griffith University, Gold Coast, Queensland, Australia

Accepted for Publication: 29 May 2019

Medicine & Science in Sports & Exercise, Publish Ahead of Print
DOI: 10.1249/MSS.0000000000002060

Individual Region- and Muscle-specific Hamstring Activity at Different Running Speeds

András Hegyi[1], Basílio AM Gonçalves[1,2], Taija Finni[1], Neil J Cronin[1]

[1]Neuromuscular Research Center, Faculty of Sport and Health Sciences, University of Jyväskylä, Jyvaskyla, Finland; [2]School of Allied Health Sciences, Griffith University, Gold Coast, Queensland, Australia

Corresponding author:

András Hegyi

LL175, P.O. Box 35, FI-40014, Jyväskylä, Finland

E-mail: andras.a.hegyi@jyu.fi

The authors have no professional relationships with companies or manufacturers who will benefit from the results of the present study. The results of the present study do not constitute endorsement by ACSM. The results of this unfunded study are presented clearly, honestly, and without fabrication, falsification, or inappropriate data manipulation.

Abstract

Introduction: Hamstring strain injuries typically occur in the proximal biceps femoris long head (BFlh) at high running speeds. Strain magnitude seems to be the primary determinant of strain injury, and may be regulated by muscle activation. In running, BFlh strain is largest in the proximal region, especially at high speeds. However, region-specific activity has not been examined. This study examined the proximal-distal and intermuscular activity of BFlh and semitendinosus (ST) as a function of increasing running speed. **Methods:** Thirteen participants ran at steady speeds of 4.1 (slow), 5.4 (moderate), and 6.8 $m \cdot s^{-1}$ (fast) on a treadmill. Region- and muscle-specific electromyography (EMG) activity were recorded at each speed using high-density EMG, and were normalised to maximal voluntary isometric activity (MVIC). Muscle-tendon unit (MTU) lengths were calculated from kinematic recordings. Speed-effects, regional and intermuscular differences were tested with Statistical Parametric Mapping. **Results:** With increasing running speed, EMG activity increased in all regions of both muscles to a similar extent in the clinically relevant late swing phase. Increases in MTU lengths in late swing as a function of running speed were comparatively small. In fast running, EMG activity was highest in late swing in all regions, and reached 115 ±20% (proximal region, mean ±95% confidence limit), 106 ±11% (middle), and 124 ±16% (distal) relative to MVIC in BFlh. Regional and intermuscular EMG patterns were highly individual, but each individual maintained similar proximal-distal and intermuscular EMG activity patterns across running speeds. **Conclusion:** Running is associated with highly individual hamstring activity patterns, but these patterns are similar across speeds. It may thus be crucial to implement running at submaximal speeds early after hamstring injury for restoration of normal neuromuscular function.

Keywords: electromyography; biceps femoris; semitendinosus; muscle mechanics; injury mechanism; locomotion; proximal-distal differences

1 Introduction

Hamstring strain is a very common (1) and highly recurrent (1, 2) injury in running-based sports. This type of injury results in substantially decreased player availability, which negatively affects team performance (3), and leads to significant financial loss for teams (4). It seems that injury incidence has not decreased over the past few decades (1), but further understanding of injury mechanisms would likely help to reduce hamstring injury risk.

Over 80% of running-based hamstring injuries occur in the biceps femoris long head (BFlh), and only a few injuries are located in other bi-articular hamstring muscles (semitendinosus, ST, and semimembranosus, SM) (5). Anatomical and functional differences between hamstring muscles may partly explain the imbalanced intermuscular distribution of hamstring injuries. For example, the pennate architecture of BFlh suggests that it is suited to high force production rather than the rapid length changes that likely occur in high-speed running, contrary to the parallel-fibred ST (6), and these muscles also present different moment arm lengths. To reveal functional differences between muscles, muscle-tendon behaviour has been widely examined in high-speed running. Most of these studies show higher strain in BFlh than ST and SM (7–9), and high forces (10–13) acting along the lengthening BFlh muscle-tendon unit (MTU) in the late swing phase (10, 12). Although these results may explain why BFlh is particularly susceptible to injury, intermuscular coordination also seems to be important. Although bi-articular hamstrings seem to act as synergist muscles in running (14), different muscles and regions show distinct innervation patterns, which also show large inter-individual variability (6), potentially allowing for individual muscle- and region-specific activity patterns. As an example for the practical importance of intermuscular coordination between hamstring heads, ST, which shares a common

proximal tendon with BFlh (6), has been suggested to protect BFlh from injury (15). Both ST and BFlh electromyography (EMG) activity increase with increasing running speed, but differences in EMG activity between these muscles are unclear in the clinically relevant phases of the running stride, i.e. late swing and early stance (11, 16–18). Based on animal models, highly activated muscles are more protected against strain injury compared to less activated muscles (19). Thus, strain and muscle activity may be important determinants of hamstring injury risk.

Recent studies have demonstrated that both strain (20) and muscle activity (21) can vary substantially within hamstring muscles. Anatomical variations along the BFlh are large (22), leading to higher strain in the proximal compared to other muscle regions in running, especially at high running speeds (20). Correspondingly, most BFlh injuries occur near the proximal muscle-tendon junction (23). Proximal-distal variations in metabolic (24) and EMG activity (21, 25) in BFlh and ST are also considerable in several hamstring exercises. This suggests that proximal-distal variations should always be considered when examining hamstring function. Previous EMG studies only recorded from a small muscle region when examining the interplay between BFlh and ST in running, ignoring possible proximal-distal differences (11, 16–18). The existence of proximal-distal differences could affect the interpretation of hamstring activity based on a small region of the muscle (21).

Hamstring EMG studies generally report group results and, as mentioned above, show no clear differences between BFlh and ST activity in running. The inability to detect differences between muscles at the group level may arise from individual variations in the activity patterns of hamstring muscles (26). Large inter-individual differences in the relative activity of hamstring

muscles have been found recently during isometric contractions, and these differences seem to affect muscle performance (27). It is currently unknown whether individual variations in proximal-distal and intermuscular hamstring EMG patterns are evident in running.

In this study, the primary aim was to examine the impact of increasing running speed on proximal-distal and intermuscular EMG activity of the BFlh and ST muscles. An additional study aim was to examine BFlh and ST MTU length changes, allowing muscle-specific EMG activity to be interpreted in relation to muscle mechanics. We hypothesized that, with increasing speed, a general increase in hamstrings activity would occur with comparably smaller changes in MTU strains. We also hypothesized that, at the group level, BFlh activity would generally be lowest in the proximal region, as is the case in many hamstring exercises (21, 25). Moreover, we expected increasing running speed to increase regional differences within BFlh. Nonetheless, we expected individual intermuscular and proximal-distal activity patterns.

2 Methods

2.1 Participants

Participants from sports with high hamstring injury prevalence (football and Gaelic football) were recruited from local clubs. Exclusion criteria were previous hamstring and anterior cruciate ligament injuries, as well as recent (<6 months) lower body injuries and any current injury or illness. A total of 13 male participants (mean ± standard deviation, age: 25 ± 3 years, height: 1.80 ± 0.07 m, body mass: 79 ± 9 kg, preferred kicking leg: 3 left, 10 right) volunteered for this study. Participants were fully informed of the procedures and risks and gave written informed

consent before participating in the testing procedures. Study procedures were approved by the local ethics committee and were performed according to the Declaration of Helsinki.

Sample size was defined based on an *a priori* sample size calculation, with the goal of detecting expected regional differences in BFlh and ST. Since no such data are available from running, calculations were based on regional differences in the Nordic hamstring exercise (28), as this exercise requires similar hamstrings activity to that expected in running at the target running speeds (17). Cohen's *d* differences between proximal and distal regions in Nordic hamstring exercise ranged between 0.87 – 1.25 (BFlh) and 0.87 – 1.41 (ST). Therefore, we aimed to observe differences of $d = 0.85$ with 80% power ($\alpha = 0.05$).

2.2 Study design

The study consisted of two sessions with 4-7 days in-between. The first session started with a standardized warm-up consisting of whole-body mobilisation, five minutes jogging at self-selected speed, and running at increasingly faster speeds of 3.3 $m \cdot s^{-1}$, 4.4 $m \cdot s^{-1}$, 5.6 $m \cdot s^{-1}$, and 6.7 $m \cdot s^{-1}$ (~15 strides per leg per speed) on a motorized treadmill (University of Jyväskylä, Finland; maximum treadmill speed: 13.9 $m \cdot s^{-1}$). This was followed by a maximum running speed test on the same treadmill. Participants wore regular cushioned running shoes and a safety harness whenever running on the treadmill. The harness was fixed to an electric system that stopped the treadmill in the event of a fall. An additional emergency button was held by the participant while running. Each participant tested this safety system to ensure that they were not afraid of running at their maximum speed on the treadmill. To test maximum running speed, an investigator increased the speed of the treadmill gradually from 1.4 $m \cdot s^{-1}$ until the participant stopped the treadmill or fell due to technical failure. Speed increments were steeper at slower speeds and

then slowed down to ~0.2 $m \cdot s^{-1}$ per second close to maximum speed. The highest speed reached without clear technical failure was estimated based on video recordings. This test was performed three times, with four-minutes rest periods in-between, and the highest speed of all three trials was defined as the maximum individual running speed. Thereafter, participants practiced maximum isometric knee flexion contractions (MVICs), which were used in the main testing session for normalisation.

In the main testing session, high-density electromyography (HD-EMG) preparation and the warm-up protocol were followed by MVICs in a custom-made knee flexion force measuring device (21). MVICs were performed lying prone with neutral trunk, neutral hips and the left knee flexed to 30°. The right leg was extended and hips were firmly fixed to the measurement device. We asked participants to gradually increase knee flexion contraction intensity in the left leg up to 100% MVIC over ~2-3 seconds, and then maintain MVIC for two seconds. Three repetitions were performed with two-minutes rest periods in-between. Reflective markers and force-sensitive resistors were then mounted on the participants to define lower body kinematics and event timings in running, respectively. Based on pilot testing, 75% of maximum running speed was as close to the maximum speed as possible while allowing~15 strides per leg without clear technical failure. This speed was thus chosen as the fastest testing speed, to maximise the chance of obtaining reliable EMG signals and minimise fatigue. In addition to 75% of maximum running speed, participants ran at 45% and 60% of maximum running speed to allow the effects of speed to be examined from the EMG data. Hereafter, these speeds are referred to as ‘fast’, ‘slow’, and ‘moderate’ speeds, respectively. Just before data collection in running, each target speed was practiced (slow, moderate, and fast speeds, in order) with four-minutes rest in-between. To practice, the investigator gradually increased the speed of the treadmill from

walking speed (~1.4 $m \cdot s^{-1}$) up to the target speed within ten seconds, which was maintained for at least 15 strides per leg, after which the treadmill was slowed down to a complete stop. For actual data collection, the same three speeds were then repeated in random order with four-minutes rest periods. Due to laboratory setup restrictions, kinematics and EMG were only recorded from the left leg for all individuals.

2.3 Data collection

2.3.1 Proximal-distal electromyography activity

Participants lay prone with neutral trunk, hip and knee angles for HD-EMG preparation. Sixteen-electrode HD-EMG arrays (10 mm inter-electrode distance, OT Bioelettronica, Torino, Italy) were attached over each of the BFlh and ST muscles (Figure 1). First, we defined the borders of each muscle, the position of the ST tendinous inscription (6), and the distal muscle-tendon junctions (in flexed knee position) using B-mode 2D ultrasonography (EchoBlast 128, Telemed Inc., Vilnius, Lithuania). The skin was then shaved, abraded and cleaned with alcohol to decrease skin impedance. HD-EMG arrays were attached along each muscle so that they were as far away from the muscle borders as possible to minimise cross-talk from neighbouring muscles. To standardize proximal-distal positioning for BFlh, channel 8-9 from the distal end was aligned with 50% of the length between the ischial tuberosity and the popliteal fold. For ST, the array was placed 1 cm below the tendinous inscription, which is an anatomical landmark defining two distinct regions of the muscle. Due to the long distal tendon of ST, we also ensured that the most distal electrode was still proximal to the distal muscle-tendon junction. The arrays were attached using double-sided tape. Electrode cavities were filled with 20 µL conductive gel (Signa gel, Parker Laboratories, NJ, USA), then further secured with adhesive tape to minimise movement

artefacts. A reference electrode strap was secured around the right wrist. Arrays were connected to an A/D converter (12-bit, OT Bioelettronica), amplified (x1000), and digital signals were recorded in BioLab software (v 3.1, OT Bioelettronica). Signal quality was checked visually during submaximal knee flexions. Fifteen differential EMG channels were recorded for each muscle at 2048 Hz sampling frequency.

2.3.2 MVICs for normalisation

During MVICs, an ankle strap placed above the lateral malleolus of the left leg was connected to the strain gauge of the measurement device. Force signals were amplified (x1000) and digitised (A/D converter, Cambridge Electronic Designs, Cambridge, UK) to record at 1000 Hz using Spike2 software (Cambridge Electronic Desings). A digital synchronisation signal was sent from Spike2 to BioLab to synchronise force and HD-EMG recordings.

2.3.3 Kinematics

To estimate hip and knee angular displacements and calculate muscle-tendon length changes in running, lower body kinematics were recorded with a 7-camera 3-D motion analysis system (VICON Inc., Oxford, UK). Reflective markers were mounted on the pelvis and left leg according to the plug-in gait model: anterior and posterior superior iliac spines on both sides, lateral surface of the thigh, flexion-extension axis of the knee, lateral surface of the shank, lateral malleolus, and over the calcaneus and second metatarsal head. Foot markers were placed on the left shoe. Marker displacements were recorded at 250 Hz in Nexus software (v2.5, VICON Inc.). To estimate segment lengths, joint centres, and joint coordinates, a standing trial was recorded prior to recording marker displacements in running.

2.3.4 Contact timing

To define foot contact timings, four force-sensitive resistors were taped to the sole of the left foot under the big toe, the head of the first and fifth metatarsal joints, and the heel, respectively. Analogue force signals were digitised and recorded at 1000 Hz in Spike2. To synchronise all signals, a digital signal was sent from Spike2 to the BioLab and Nexus software.

2.4 Data analysis

2.4.1 High-density electromyography

A few EMG channels were excluded from the analysis due to array malfunctions. For BFlh a total of 11 ± 1 (median ± interquartile range) channels were analysed (proximal region: 4 ± 1, middle: 3 ± 2, distal: 4 ± 1). For ST, a total of 11 ± 2 channels were analysed (proximal: 4 ± 2, middle: 3 ± 1, distal: 4 ± 2). EMG signals were offline band-pass (20-500 Hz) and notch (50 Hz) filtered with a 4^{th} order zero-lag Butterworth filter, and then rectified in Matlab (MathWorks Inc., Natick, MA, USA). For MVICs, average EMG activity was defined for a 1-second stable plateau around peak torque. For each EMG channel and muscle, the highest MVIC activity was chosen for normalisation.

To smooth the signals for curve analyses, a 10-Hz low-pass zero-phase Butterworth filter was applied to each channel. Similar to the approach we used previously, the proximal, middle, and distal five channels of each array were averaged to estimate the EMG activity levels in different muscle regions (21, 25). Additionally, all functioning channels were averaged along each muscle to estimate the overall activity level of each muscle. Averaging several channels was performed to minimise the effects of muscle shift under the electrodes on EMG amplitudes. Foot strike (FS)

and toe-off (TO) timings were defined based on the sum of all four force-sensitive resistors, i.e. increasing (FS) or decreasing (TO) force for 20 consecutive frames. Then, EMG curves for each muscle and region were time-normalised for each stride (from FS until the next FS) and then averaged for each running speed and individual. These curves were included in the statistical analysis.

2.4.2 Muscle-tendon lengths and stride sub-phases

Marker trajectories were smoothed with a 10 Hz low-pass Butterworth filter, and hip and knee joint angles were then calculated in Nexus software applying the plug-in gait model. Sagittal plane hip and knee angles were exported and used to calculate BFlh and ST MTU lengths relative to thigh length (29) using Matlab. MTU lengths were calculated for each stride, time-normalised, then corresponding time-points across strides were averaged for each running speed and individual. Additionally, joint angles and contact timings were used to define stride sub-phases as (1) early stance (from FS to maximum knee angle in stance), (2) late stance (from maximum knee angle in stance to TO), (3) early swing (from TO to maximum knee angle in swing), (4) mid swing (from maximum knee angle in swing to maximum hip flexion angle), and (5) late swing (from maximum hip flexion angle to ipsilateral FS) (16). The number of strides defined and analysed were 19 ± 3, 18 ± 2, and 17 ± 3 (median ± interquartile range) at slow, moderate, and fast running speeds, respectively.

2.4.3 Inter-individual differences

To quantify inter-individual differences in EMG activity and MTU lengths, inter-individual coefficients of variation (CV%) were calculated for each muscle's EMG activity (all channels

averaged), for each region of BFlh and ST, and for MTU lengths. Additionally, to see whether inter-individual variability in intermuscular coordination changed across the stride and between speeds, coefficients of variation were calculated for BFlh activity relative to ST activity (i.e. BFlh-to-ST ratio) for each speed. All CV%s were calculated for each sub-phase of the stride.

2.4.4 Statistical analysis

To compare curves with high temporal resolution, all statistical analyses were performed using Statistical Parametric Mapping (SPM (30), v0.4, www.spm1d.org) in Matlab. Two-way repeated measures ANOVAs were run across the time-normalised running strides. SPM{F} test statistics were calculated to test speed x regional EMG interactions (for each muscle), speed x muscle-specific EMG interactions, and speed x MTU length interactions. Family-wise type I error rate was set at 0.05. In case of an interaction at any time-point across the stride, locations of the differences were tested using paired-sample t-tests with Bonferroni correction. In all SPM analyses, the test statistic (SPM{F} or SPM{t}) was calculated first, and the critical threshold (F* or t*) was then defined based on Random Field Theory so that only α% of random curves were expected to exceed the critical threshold in the long run. Whenever the test statistic trajectory crossed the critical threshold (forming so-called supra-threshold clusters) the difference was deemed statistically significant. Finally, p values were calculated for each supra-threshold cluster. SPM technical details are described elsewhere (30, 31).

3 Results

The maximum running speed was 9.04 ± 0.52 $m \cdot s^{-1}$ (mean ± standard deviation). Thus, data were collected at speeds of 4.07 ± 0.23, 5.42 ± 0.31 and 6.78 ± 0.39 $m \cdot s^{-1}$ (slow, moderate, and fast speeds, respectively).

When all channels along each muscle were averaged, peak BFlh EMG amplitudes were observed in late swing and were 63 ±9% (mean ±95% confidence limit, slow running speed), 90 ±11% (moderate), 115 ±13% (fast) relative to MVIC. Peak ST EMG activity values in late swing were 69 ±9% (slow), 102 ±28% (moderate), 121 ±18% (fast) relative to MVIC. Group means ± standard deviations across the stride are shown for each speed in Figure 2. A speed x muscle EMG interaction was only seen in a short period before toe-off (25-29% stride, $p = 0.025$). Post-hoc analyses showed no difference between muscles at any speed across the stride [see Figure, Supplemental Digital Content 1, Upper panels show mean and standard deviation (s.d.) of biceps femoris long head (BFlh) and semitendinosus (ST) electromyography (EMG) activity (normalised to maximal voluntary isometric contraction, MVIC) at slow, moderate and fast running speeds. Lower panels represent corresponding SPM{t} test statistic trajectories (thick black lines), http://links.lww.com/MSS/B641].

Speed x MTU length interactions were found in late stance (23-28% stride, $p = 0.035$) and in swing (33-83% and 93-100% stride, $p < 0.001$ and $p = 0.027$). In both muscles, increasing speed increased the total length changes, mainly due to a decrease in minimum MTU lengths [$p < 0.001$; see Figure, Supplemental Digital Content 2, Effects of running speed on muscle-tendon unit (MTU) lengths, http://links.lww.com/MSS/B642]. Maximum lengths only increased from slow to moderate speed but not from moderate to fast speed (see Figure, Supplemental Digital

Content 2, http://links.lww.com/MSS/B642). BFlh MTU was significantly longer than ST MTU across the entire stride at all speeds ($p < 0.001$) (Figure 2). Individual MTU length changes were similar across participants [see Figure, Supplemental Digital Content 3, Similar patterns between individuals S1-S13 in biceps femoris long head (BFlh) and semitendinosus (ST) muscle-tendon unit (MTU) lengths, http://links.lww.com/MSS/B643], resulting in inter-individual CVs as small as 1-3% across speeds in both muscles [see Figure, Supplemental Digital Content 4, Inter-individual coecients of variations in muscle-tendon unit lengths in the early stance (ESt), late stance (LSt), early swing (ESw), mid swing (MSw), and late swing (LSw); http://links.lww.com/MSS/B644].

3.1. Regional EMG activity

Group mean EMG amplitudes defined proximal-distally along each muscle are shown in Figure 1.

In BFlh, the highest EMG activity was reached in late swing in all muscle regions. After dividing each muscle into three distinct regions, region-specific peak activity levels in BFlh in slow running were 58 ±9% (proximal region; mean ±95% confidence limit), 63 ±8% (middle), and 69 ±11% (distal) relative to MVIC. At moderate speed, the corresponding values were 93 ±16%, 86 ±9%, and 94 ±14%, respectively. At fast speed, EMG peak values were 115 ±20% (proximal), 106 ±11% (middle), and 124 ±16% (distal) relative to MVIC.

In BFlh, a speed x region interaction was found only in early swing (41-56% stride, $p < 0.001$). With increasing speed, EMG activity increased in all BFlh regions across the stride ($p < 0.001$) except in late stance (proximal: 20-29% middle: 16-30%, and distal: 17-29% stride,

respectively). Differences between speeds are shown for each region in Figure 3. Post hoc analyses showed no differences between muscle regions at any running speed at any time point across the stride [see Figure, Supplemental Digital Content 5, Regional differences in the electromyography (EMG) activity of biceps femoris long head (BFlh, normalised to maximal voluntary isometric contraction, MVIC); http://links.lww.com/MSS/B645.].

In ST, the highest EMG activity was reached in late swing in all muscle regions, similar to BFlh. Region-specific peak activity levels in ST in slow running were 70 ±17% (proximal region; mean ±95% confidence limit), 65 ±8% (middle), and 74 ±9% (distal) relative to MVIC. The corresponding values at moderate speed were 99 ±28%, 91 ±14%, and 113 ±46%, respectively. At fast speed, EMG peak values were 136 ±32% (proximal), 118 ±15% (middle), and 122 ±15% (distal) relative to MVIC.

In ST, similar to BFlh, a speed x region interaction was found only in early swing (52-56% stride, $p = 0.028$). With increasing speed, EMG activity increased in all ST regions across the entire stride in the proximal and middle regions ($p < 0.001$) and in most phases in the distal region (0-23%, $p < 0.001$; 25-32%, $p = 0.010$; 39-80%, $p < 0.001$; 89-100%, $p = 0.001$). Differences between speeds are shown for each region in Figure 4. No differences between muscle regions were detected at any of the running speeds [see Figure, Supplemental Digital Content 6, Regional differences in the electromyography (EMG) activity of semitendinosus (ST, normalised to maximal voluntary isometric contraction, MVIC); http://links.lww.com/MSS/B646.].

3.2 Individual EMG patterns

Individual region-specific activity patterns were evident in both BFlh (Figure 5) and ST (Figure 6; and see Figure, Supplemental Digital Content 7 [Large inter-individual coefficients of variations in regional activity levels in the early stance (ESt), late stance (LSt), early swing (ESw), mid swing (MSw), and late swing (LSw); http://links.lww.com/MSS/B647] for inter-individual coefficients of variations for each region and speed). Similar to regional patterns, the overall activity pattern of each muscle showed distinct individual patterns [see Figure, Supplemental Digital Content 8, Individual (S1-S13) muscle-specific electromyography (EMG) activity patterns of biceps femoris long head (BFlh) and semitendinosus (ST) (normalised to maximal voluntary activity, MVIC; http://links.lww.com/MSS/B648); and see Figure, Supplemental Digital Content 9, (Large inter-individual coefficients of variations in muscle activity levels at slow (4.1 ± 0.2 m·s-1), moderate (5.4 ± 0.3 m·s-1), and fast (6.8 ± 0.4 m·s-1) running speeds) for inter-individual CVs in muscle-specific EMG activity]. BFlh-to-ST EMG ratio ranged across speeds and sub-phases between 28% and 71%, depicting individual intermuscular coordination strategies (Figure, Supplemental Digital Content 9, http://links.lww.com/MSS/B649). In general, CVs were lowest in late swing at all speeds (1.6 times higher in other stride phases on average). Of all speeds, late swing CVs were smallest at the fast running speed (CV range across regions and muscles = 21-42%).

4 Discussion

In this study, we examined proximal-distal and intermuscular differences in BFlh and ST muscle activity across a range of running speeds. Contrary to our primary hypothesis, at the group level, proximal-distal and intermuscular statistical differences were not detected in BFlh or ST at any

of the running speeds. However, as expected, individual differences were evident across the entire stride at all speeds. According to our secondary hypothesis, with increasing speed, large increases in hamstring HD-EMG activity were accompanied by relatively small increases in maximum MTU lengths in the late swing phase, indicating higher hamstring stiffness at higher speeds.

Similar to previous EMG studies (11, 32), we found a substantial increase in hamstring EMG activity with increasing running speed (Figures 3-4), and the highest activity levels were observed in late swing and early stance at all speeds, as also observed previously (11, 16–18, 32). In these phases, BFlh and ST EMG activity reached a higher amplitude at 75% of maximum running speed (which is considered sprinting speed in this cohort, > 24 $km \cdot h^{-1}$) compared to that in typical hamstring exercises performed at submaximal or maximal loads (21, 25). EMG values in late swing and early stance also exceeded the muscle activity levels achieved during MVICs, as observed previously (32, 33). This reinforces the notion that it is challenging to activate hamstrings during regular exercises to the same extent as during sprinting. It should be noted that exercises are generally performed at a much slower pace relative to that of sprinting, and movement speed is known to affect EMG amplitudes (34). Our results further support the idea that in the early stance and late swing phases, high BFlh and ST EMG activities are reached at relatively long muscle lengths (11). This in turn supports the notion that exercises facilitating long hamstring operating lengths and high activation may help to prepare the hamstrings for the requirements of high-speed running (35).

The typical bi-phasic activity pattern (i.e. peaks at early stance and late swing) of BFlh and ST was seen for most individuals, and hamstring injuries seem to occur in these phases (36).

However, a third burst in the early-to-mid swing phase was seen for 6 individuals in BFlh (Figure 5) and for 3 individuals in ST (Figure 6). In this phase the hamstrings are believed to stabilize the hip and knee while these joints are being flexed and extended, respectively (17). At the same time, the rate of lengthening of the hamstring MTUs is the highest in this phase of running (Figure 2). The fusiform architecture of ST suggests that this muscle is built for such fast muscle actions (6). On the contrary, BFlh is not suited to rapid length changes (6). Rapid stretch in this phase lowers the potential for stretch relaxation, increasing tensile forces acting along the muscle (37). MTU strain was relatively constant across individuals, contrary to the large inter-individual variation of BFlh activity during this lengthening phase. According to Garrett et al. (19), increasing muscle activity increases the energy absorbed by the muscle during lengthening and decreases strain injury risk. If this applies to hamstrings in sprinting, increased BFlh activity could be a protective mechanism against muscle strain injury. However, increasing muscle activity (and thus stiffness) generally results in more of the MTU stretch being transferred to the aponeuroses and tendons (38), which are often involved in hamstring strain injuries. It is likely that there is an optimal range of BFlh activity in running, and that this optimum range is influenced by individual factors such as the mechanical properties and architecture of the hamstring muscle components. This could partly explain individual variations in BFlh activity in running. Although hamstring injuries seem to occur mainly in late swing, structural damage potentially accumulating in mid swing may predispose the BFlh to strain injury in late swing, where large tensile forces act at long hamstring lengths. Future studies should further examine the link between the magnitude of BFlh activity in these phases and strain injury risk.

BFlh EMG activity is likely affected by the activity of other synergist muscles like ST. BFlh-to-ST activity ratio showed large individual variability, suggesting individual strategies for the

relative activation of these muscles in running and sprinting. Statistical differences were not seen between BFlh and ST activity. However, the lack of detectable difference seems to result from large individual variations (Figure, Supplemental Digital Content 3, http://links.lww.com/MSS/B643). It seems that a similar magnitude of activity between hamstring muscles may be advantageous for muscle performance in isometric fatiguing contractions (27), and may be associated with decreased hamstring injury risk (15). It is currently unclear whether this directly implies that all individuals should activate these muscles similarly in running. Individual coordination strategies in running may require individual muscle-specific hamstring strengthening. For example, some may benefit from BFlh-dominant exercises such as 45° hip extension on a roman chair (25), while others may benefit more from ST-dominant exercises such as Nordic hamstring exercise performed with flexed hips (39) to achieve different adaptations. Morphological and architectural characteristics of the hamstring muscles show substantial individual variations (40), and it should be clarified whether these variations are linked to individual coordination strategies.

Aside from intermuscular variations, proximal-distal activity patterns were also highly specific to individuals, which may be the reason why regional differences were not statistically different when all individuals were pooled together for statistical analysis. Regional activity patterns may be associated with regional adaptations, although we are not aware of studies examining this phenomenon in hamstrings. Within the BFlh, it seems to be challenging to selectively activate the proximal region (the region where most injuries occur) via hamstring exercises (21, 25). Nonetheless, in the current study, one participant showed the highest activity in the proximal BFlh relative to other muscle regions in running (S11 in Figure 5) and some others showed similar proximal EMG activity to other regions (S2, S4, S6 in Figure 5). It may be that for some

individuals, potential regional adaptations gained through hamstring exercises may not be optimal to prepare the proximal region for the needs of high-speed running. Defining hamstring activity patterns for each player in a team could assist exercise selection, however the cost-benefit balance of this approach is currently unclear. Examining the link between individual patterns in running vs in hamstring exercises may help to improve exercise selection for hamstring injury risk reduction.

Since hamstring injuries typically occur at high running speeds, speed-dependent changes in intermuscular activity may be important to note. One study (17) showed that BFlh-to-ST activity ratio increased in the late swing phase with increasing running speed. On the contrary, we did not detect speed effects on intermuscular EMG activity patterns. Individual muscle-specific (and region-specific) activity patterns were similar across a range of running speeds. This supports the idea that early implementation of running, even at slow speeds, might be crucial to restore the neuromuscular function of the hamstring muscles after a hamstring injury.

Similar to previous studies (11, 12), we observed large increases in hamstring activity with increasing running speed without substantial changes in peak MTU lengths in late swing, implying higher MTU stiffness at higher speeds. Although the BFlh and ST MTUs undergo a stretch-shortening cycle throughout the running stride, muscle-tendon decoupling likely occurs to some extent. Based on simulations, increasing muscle activity from early to late swing slows the stretch of the BFlh muscle component, and the tendons take up part of the MTU lengthening (10). Individual variations in muscle activity in swing imply that muscle-tendon decoupling may also be individual-specific. Although the compliance of the series elastic elements affects the length change of the muscle component, even highly compliant tendons seem to require the

muscle component to bear most of the MTU lengthening within the BFlh (10). Although it has recently been suggested that the fascicles of the BFlh are quasi-isometric in late swing (41), this has not been supported with experimental data. We recently attempted to assess BFlh fascicle behaviour and relate that to muscle-tendon behaviour in running *in vivo*, using a combination of B-mode 2-D ultrasonography and kinematic analysis. However, we were unable to quantify fascicle length changes due to out-of-plane fascicle rotations (see Video, Supplemental Digital Content 10, example ultrasound recordings in locomotion, http://links.lww.com/MSS/B650). Fascicle length changes appear to be significant throughout the stride but accurately quantifying these changes remains challenging. According to magnetic resonance imaging-based modelling, a further challenge is that BFlh strain seems to be heterogeneous within the muscle in running, with the highest strain near the proximal muscle-tendon junction, where most injuries occur (20). Heterogeneous proximal-distal strain distribution may be associated with heterogeneous proximal-distal EMG activity patterns observed in the current study. Further technical improvements are needed to fully understand the association between BFlh muscle activity and muscle-tendon mechanics in running.

Although this study focused solely on BFlh and ST, it is likely that large inter-individual variations are also affected by individual contributions of other muscles. For example, modelling data suggest that several muscles in the lumbo-pelvic region affect BFlh behaviour in running (12). Further experimental data suggest that an increased activation of the gluteus maximus in running can decrease hamstring strain injury risk (42), which seems to be more pronounced in fatigued conditions (43). Our results suggest that these factors should be examined at an individual level in future studies to understand the interplay between muscles in running.

It is important to note some limitations of this study. An inherent limitation of surface EMG methods is the contamination of the signals by neighbouring muscle activity (i.e. cross-talk). To limit this effect, we attached the electrode arrays as far from the borders of the target muscle as possible (defined with ultrasonography), and applied short inter-electrode distances (10 mm) and electrodes with a small pick-up area. Since the subcutaneous layer over the hamstrings is generally thicker in females than in males (increasing the potential for cross-talk) we measured male athletes only. The EMG results might have been affected by the EMG normalisation method, although changes with increasing speed are not affected by this factor. It should also be noted that muscle-tendon length calculations are slightly affected by the model used and the cut-off frequency applied, although MTU behaviour was not the main focus of this study. Furthermore, we measured at submaximal (and not at maximal) running speeds, due to the methodological constraints previously mentioned. However, the fastest running speed used in this study is already considered sprinting in football codes. It remains unclear though whether higher sprinting speeds would result in different hamstring activity patterns from what we observed. Notably, running trials were performed on a motorized treadmill to ensure that the target speeds were reached and maintained across several strides. However, differences between hamstring activation and mechanics when running on a treadmill vs. overground are yet to be clarified. We also emphasize that we recruited amateur athletes, so the results may not be applicable to other populations.

To summarize the main findings of this study, hamstring intermuscular and proximal-distal activity patterns seem to be highly variable between individuals, but are qualitatively consistent within individuals across a range of running speeds. This means that slow-speed running results in a similar shaped activity pattern to high-speed running, and thus should be applied early after

a hamstring injury to facilitate neuromuscular recovery and prepare for high-speed running. Future studies should examine how fatigue affects hamstring activity patterns, and whether individual differences in hamstring coordination are linked to performance and hamstring injury susceptibility in running.

5 Conflict of interest

The authors have no professional relationships with companies or manufacturers who will benefit from the results of the present study. The results of the present study do not constitute endorsement by ACSM. The results of this unfunded study are presented clearly, honestly, and without fabrication, falsification, or inappropriate data manipulation.

6 References

1. Ekstrand J, Waldén M, Hägglund M. Hamstring injuries have increased by 4% annually in men's professional football, since 2001: A 13-year longitudinal analysis of the UEFA Elite Club injury study. *Br J Sports Med*. 2016;50(12):731–7.

2. Malliaropoulos N, Isinkaye T, Tsitas K, Maffulli N. Reinjury after acute posterior thigh muscle injuries in elite track and field athletes. *Am J Sports Med*. 2011;39(2):304–10.

3. Hägglund M, Waldén M, Magnusson H, Kristenson K, Bengtsson H, Ekstrand J. Injuries affect team performance negatively in professional football: An 11-year follow-up of the UEFA Champions League injury study. *Br J Sports Med*. 2013;47(12):738–42.

4. Hickey J, Shield AJ, Williams MD, Opar DA. The financial cost of hamstring strain injuries in the Australian Football League. *Br J Sports Med*. 2014;48(8):729–30.

5. Woods C, Hawkins RD, Maltby S, Hulse M, Thomas A, Hodson A. The Football Association Medical Research Programme: An audit of injuries in professional football - Analysis of hamstring injuries. *Br J Sports Med*. 2004;38:36–41.

6. Woodley SJ, Mercer SR. Hamstring muscles: Architecture and innervation. *Cells Tissues Organs*. 2005;179(3):125–41.

7. Schache AG, Dorn TW, Blanch PD, Brown NAT, Pandy MG. Mechanics of the human hamstring muscles during sprinting. *Med Sci Sports Exerc*. 2012;44(4):647–58.

8. Thelen DG, Chumanov ES, Hoerth DM, et al. Hamstring muscle kinematics during treadmill sprinting. *Med Sci Sports Exerc*. 2005;37(1):108–17.

9. Wan X, Qu F, Garrett WE, Liu H, Yu B. The effect of hamstring flexibility on peak hamstring muscle strain in sprinting. *J Sport Heal Sci*. 2017;6(3):283–9.

10. Thelen DG, Chumanov ES, Best TM, Swanson SC, Heiderscheit BC. Simulation of biceps femoris musculotendon mechanics during the swing phase of sprinting. *Med Sci Sports Exerc*. 2005;37(11):1931–8.

11. Schache AG, Dorn TW, Wrigley T V., Brown NAT, Pandy MG. Stretch and activation of the human biarticular hamstrings across a range of running speeds. *Eur J Appl Physiol*. 2013;113(11):2813–28.

12. Chumanov ES, Heiderscheit BC, Thelen DG. The effect of speed and influence of individual muscles on hamstring mechanics during the swing phase of sprinting. *J Biomech*. 2007;40(16):3555–62.

13. Chumanov ES, Heiderscheit BC, Thelen DG. Hamstring musculotendon dynamics during stance and swing phases of high-speed running. *Med Sci Sports Exerc*. 2011;43(3):525–32.

14. Nishida K, Hagio S, Kibushi B, Moritani T, Kouzaki M. Comparison of muscle synergies for running between different foot strike patterns. *PLoS One*. 2017;12(2):e0171535.

15. Schuermans J, Van Tiggelen D, Danneels L, Witvrouw E. Biceps femoris and semitendinosus - Teammates or competitors? New insights into hamstring injury mechanisms in male football players: A muscle functional MRI study. *Br J Sports Med*. 2014;48(22):1599–606.

16. Higashihara A, Nagano Y, Ono T, Fukubayashi T. Differences in activation properties of the hamstring muscles during overground sprinting. *Gait Posture*. 2015;42(3):360–4.

17. Higashihara A, Ono T, Kubota J, Okuwaki T, Fukubayashi T. Functional differences in the activity of the hamstring muscles with increasing running speed. *J Sports Sci*. 2010;28(10):1085–92.

18. Yu B, Queen RM, Abbey AN, Liu Y, Moorman CT, Garrett WE. Hamstring muscle kinematics and activation during overground sprinting. *J Biomech*. 2008;41(15):3121–6.

19. Garrett WE, Safran MR, Seaber A V., Glisson RR, Ribbeck BM. Biomechanical comparison of stimulated and nonstimulated skeletal muscle pulled to failure. *Am J Sports Med*. 1987;15(5):448–54.

20. Fiorentino NM, Rehorn MR, Chumanov ES, Thelen DG, Blemker SS. Computational models predict larger muscle tissue strains at faster sprinting speeds. *Med Sci Sports Exerc*. 2014;46(4):776–86.

21. Hegyi A, Péter A, Finni T, Cronin NJ. Region-dependent hamstrings activity in Nordic hamstring exercise and stiff-leg deadlift defined with high-density electromyography. *Scand J Med Sci Sport*. 2018;28(3):992–1000.

22. Kellis E, Galanis N, Natsis K, Kapetanos G. Muscle architecture variations along the human semitendinosus and biceps femoris (long head) length. *J Electromyogr Kinesiol*. 2010;20(6):1237–43.

23. Verrall GM, Slavotinek JP, Barnes PG, Fon GT. Diagnostic and prognostic value of clinical findings in 83 athletes with posterior thigh injury. Comparison of clinical findings with Magnetic Resonance Imaging documentation of hamstring muscle strain. *Am J Sports Med*. 2003;31(6):969–73.

24. Mendez-Villanueva A, Suarez-Arrones L, Rodas G, et al. MRI-based regional muscle use during hamstring strengthening exercises in elite soccer players. *PLoS One*. 2016;11(9):e0161356.

25. Hegyi A, Csala D, Péter A, Finni T, Cronin NJ. High-density electromyography activity in various hamstring exercises. *Scand J Med Sci Sport*. 2019;29(1):34–43.

26. Guidetti L, Rivellini G, Figura F. EMG patterns during running: Intra-and inter-individual variability. *J Electromyogr Kinesiol*. 1996;6(1):37–48.

27. Avrillon S, Guilhem G, Barthelemy A, Hug F. Coordination of hamstrings is individual specific and is related to motor performance. *J Appl Physiol*. 2018;125(4):1069–79.

28. Hegyi A, Péter A, Finni T, Cronin NJ. Region-dependent hamstrings activity in Nordic hamstring exercise and stiff-leg deadlift defined with high-density electromyography. *Scand J Med Sci Sport*. 2018;28(3):992–1000.

29. Hawkins D, Hull ML. A method for determining lower extremity muscle-tendon lengths during flexion/extension movements. *J Biomech*. 1990;23(5):487–94.

30. Friston KJ, Holmes a. P, Worsley KJ, Poline J-P, Frith CD, Frackowiak RSJ. Statistical parametric maps in functional imaging: A general linear approach. *Hum Brain Mapp*. 1995;2(4):189–210.

31. Adler R, Taylor J. *Random Fields and Geometry*. New York: Springer; 2007.

32. Kyröläinen H, Avela J, Komi P V. Changes in muscle activity with increasing running speed. *J Sports Sci*. 2005;23(10):1101–9.

33. van den Tillaar R, Solheim JAB, Bencke J. Comparison of hamstring muscle activation during high-speed running and various hamstring strengthening exercises. *Int J Sports Phys Ther*. 2017;12(5):718–727.

34. Bigland B, Lippold OCJ. The relation between force, velocity and integrated electrical activity in human muscles. *J Physiol*. 1954;123(1):214–224.

35. Askling CM, Tengvar M, Thorstensson A. Acute hamstring injuries in Swedish elite football: A prospective randomised controlled clinical trial comparing two rehabilitation protocols. *Br J Sports Med*. 2013;47(15):953–9.

36. Chumanov ES, Schache AG, Heiderscheit BC, Thelen DG. Hamstrings are most susceptible to injury during the late swing phase of sprinting. *Br J Sports Med*. 2012;46(2):90.

37. Taylor DC, Dalton JD, Seaber A V., Garrett WE. Viscoelastic properties of muscle-tendon units: The biomechanical effects of stretching. *Am J Sports Med*. 1990;18(3):300–9.

38. Cronin NJ, Peltonen J, Ishikawa M, et al. Effects of contraction intensity on muscle fascicle and stretch reflex behavior in the human triceps surae. *J Appl Physiol*. 2008;105:226–32.

39. Hegyi A, Lahti J, Giacomo J-P, Gerus P, Cronin NJ, Morin JB. Impact of hip flexion angle on unilateral and bilateral Nordic hamstring exercise torque and high-density electromyography activity [Internet]. *J Orthop Sport Phys Ther*. 2019; doi:10.2519/jospt.2019.8801.

40. Ward SR, Eng CM, Smallwood LH, Lieber RL. Are current measurements of lower extremity muscle architecture accurate? *Clin Orthop Relat Res*. 2009;467(4):1074–82.

41. Van Hooren B, Bosch F. Is there really an eccentric action of the hamstrings during the swing phase of high-speed running? part I: A critical review of the literature. *J Sports Sci*. 2017;35(23):2313–21.

42. Schuermans J, Danneels L, Van Tiggelen D, Palmans T, Witvrouw E. Proximal Neuromuscular Control Protects Against Hamstring Injuries in Male Soccer Players: A

Prospective Study with Electromyography Time-Series Analysis during Maximal Sprinting. *Am J Sports Med*. 2017;45(6):1315–25.

43. Edouard P, Mendiguchia J, Lahti J, et al. Sprint Acceleration Mechanics in Fatigue Conditions: Compensatory Role of Gluteal Muscles in Horizontal Force Production and Potential Protection of Hamstring Muscles [Internet]. *Front Physiol*. 2018; doi:10.3389/fphys.2018.01706.

Figure Captions

Figure 1. Positioning of the high-density electromyography (EMG) arrays, and group mean (N=13) proximal-distal electromyography activity levels normalised to maximum voluntary isometric (MVIC) amplitudes. Fifteen differential channels were recorded along each muscle using high-density EMG arrays (10 mm inter-electrode distance) at slow (4.1 ± 0.2 $m \cdot s^{-1}$), moderate (5.4 ± 0.3 $m \cdot s^{-1}$), and fast (6.8 ± 0.4 $m \cdot s^{-1}$) running speeds. Running stride sub-phases were defined as early stance (ESt), late stance (LSt), early swing (ESw), mid swing (MSw), and late swing (LSw).

Figure 2. Group mean and standard deviation (s.d.) of joint angular displacements, biceps femoris long head (BFlh) and semitendinosus (ST) muscle-tendon unit (MTU) lengths, and electromyography (EMG) activity (all EMG channels averaged per muscle; normalised to a maximum voluntary isometric contraction, %MVIC) at slow, moderate, and fast running speeds (4.1 ± 0.2 $m \cdot s^{-1}$, 5.4 ± 0.3 $m \cdot s^{-1}$, and 6.8 ± 0.4 $m \cdot s^{-1}$, respectively). Vertical dashed lines define the sub-phases of the running stride (0-100%) as: early stance (ESt, foot strike at 0% to maximum knee angle in stance), late stance (LSt, maximum knee angle in stance to toe-off), early swing (ESw, toe-off to maximum knee angle in swing), mid swing (MSw, maximum knee angle in swing to maximum hip angle in swing), and late swing (LWs, maximum hip angle in swing to foot strike at 100%).

Figure 3. Effects of running speed on the electromyography (EMG) activity of biceps femoris long head (BFlh) muscle regions (normalised to maximal voluntary isometric contraction, MVIC). Panels (A), (B), and (C) represent group mean and standard deviation (s.d.) across the

stride cycle at different speeds for each region. Panels (D) to(L) show the statistical parametric maps. (D), (E), and- (F) show differences between moderate (5.4 ± 0.3 $m \cdot s^{-1}$) and slow (4.1 ± 0.2 $m \cdot s^{-1}$) running speeds, (G), (H), and(I) show differences between fast (6.8 ± 0.4 $m \cdot s^{-1}$) and slow running speeds, (J), (K), and (L) show differences between fast and moderate running speeds, in the proximal, middle, and distal regions, respectively. Thick black lines are the SPM{t} test statistics representing the magnitude of the differences relative to the s.d. and sample size (N=13). Critical thresholds (t*) were calculated for each comparison after Bonferroni correction (dashed red horizontal lines; family-wise $\alpha = 0.05$). Probability (p) values are shown for each supra-threshold cluster depicting statistically significant differences. Running stride sub-phases were defined as early stance (ESt), late stance (LSt), early swing (ESw), mid swing (MSw), and late swing (LSw).

Figure 4. Effects of running speed on the electromyography (EMG) activity of semitendinosus (ST) muscle regions (normalised to maximal voluntary isometric contraction, MVIC). Panels (A), (B), and (C) represent group mean and standard deviation (s.d.) across the stride cycle at different speeds for each region. Panels (D) to(L) show the statistical parametric maps. (D), (E), and- (F) show differences between moderate (5.4 ± 0.3 $m \cdot s^{-1}$) and slow (4.1 ± 0.2 $m \cdot s^{-1}$) running speeds, (G), (H), and(I) show differences between fast (6.8 ± 0.4 $m \cdot s^{-1}$) and slow running speeds, (J), (K), and (L) show differences between fast and moderate running speeds, in the proximal, middle, and distal regions, respectively. Thick black lines are the SPM{t} test statistics representing the magnitude of the differences relative to the s.d. and sample size (N=13). Critical thresholds (t*) were calculated for each comparison after Bonferroni correction (dashed red horizontal lines; family-wise $\alpha = 0.05$). Probability (p) values are shown for each supra-threshold

cluster depicting statistically significant differences. Running stride sub-phases were defined as early stance (ESt), late stance (LSt), early swing (ESw), mid swing (MSw), and late swing (LSw).

Figure 5. Individual (rows S1-S13) region-specific biceps femoris long head (BFlh) electromyography (EMG) activity patterns normalised to maximal voluntary activity (MVIC) at slow (4.1 ± 0.2 $m \cdot s^{-1}$), moderate (5.4 ± 0.3 $m \cdot s^{-1}$), and fast (6.8 ± 0.4 $m \cdot s^{-1}$) running speeds. Note that scaling of the y axis is optimised for each individual so that regional differences are easier to identify within each individual. Foot strike is at 0% and 100% of the stride.

Figure 6. Individual (rows S1-S13) region-specific semitendinosus (ST) electromyography (EMG) activity patterns when normalised to maximal voluntary activity (MVIC) at slow (4.1 ± 0.2 $m \cdot s^{-1}$), moderate (5.4 ± 0.3 $m \cdot s^{-1}$), and fast (6.8 ± 0.4 $m \cdot s^{-1}$) running speeds. Note that scaling of the y axis is optimised for each individual so that regional differences are easier to identify within each individual. Foot strike is at 0% and 100% of the stride.

List of Supplemental Digital Content

Figure, Supplemental Digital Content 1.pdf

Figure, Supplemental Digital Content 2.pdf

Figure, Supplemental Digital Content 3.pdf

Figure, Supplemental Digital Content 4.pdf

Figure, Supplemental Digital Content 5.pdf

Figure, Supplemental Digital Content 6.pdf

Figure, Supplemental Digital Content 7.pdf

Figure, Supplemental Digital Content 8.pdf

Figure, Supplemental Digital Content 9.pdf

Video, Supplemental Digital Content 10.mp4

Figure 1

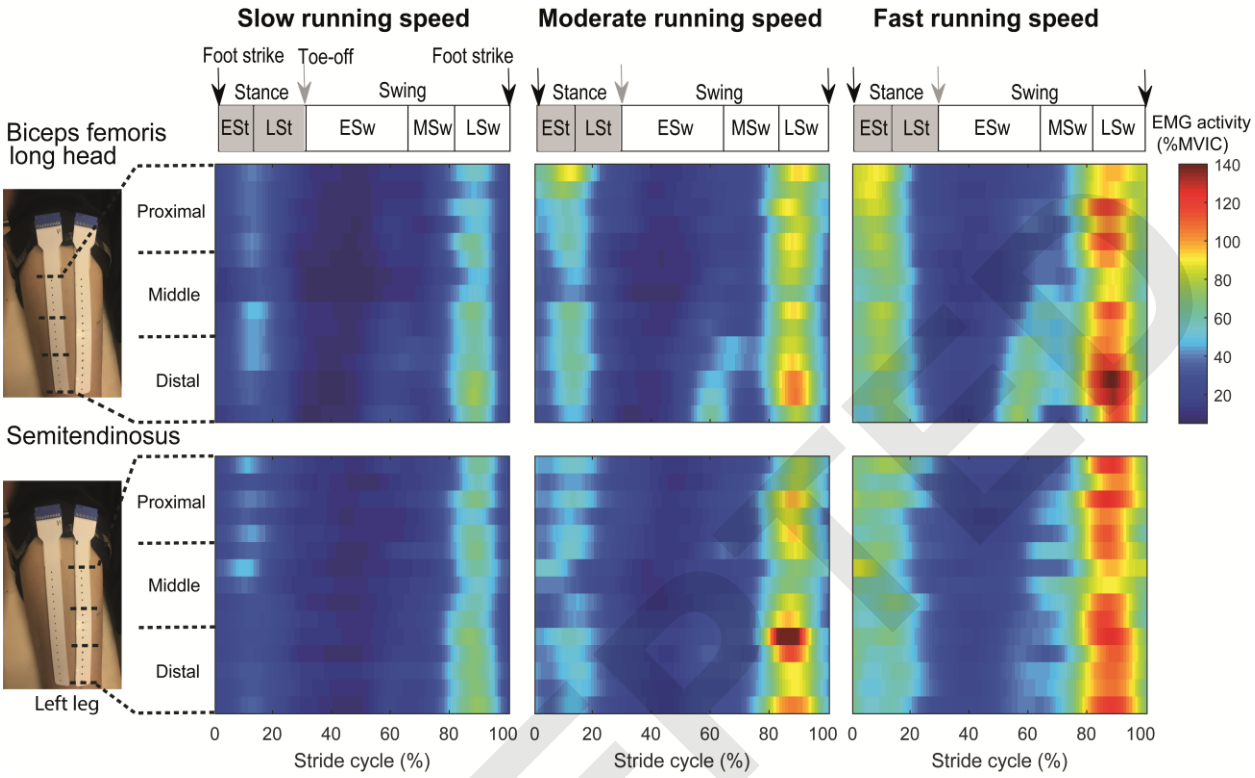

Figure 2

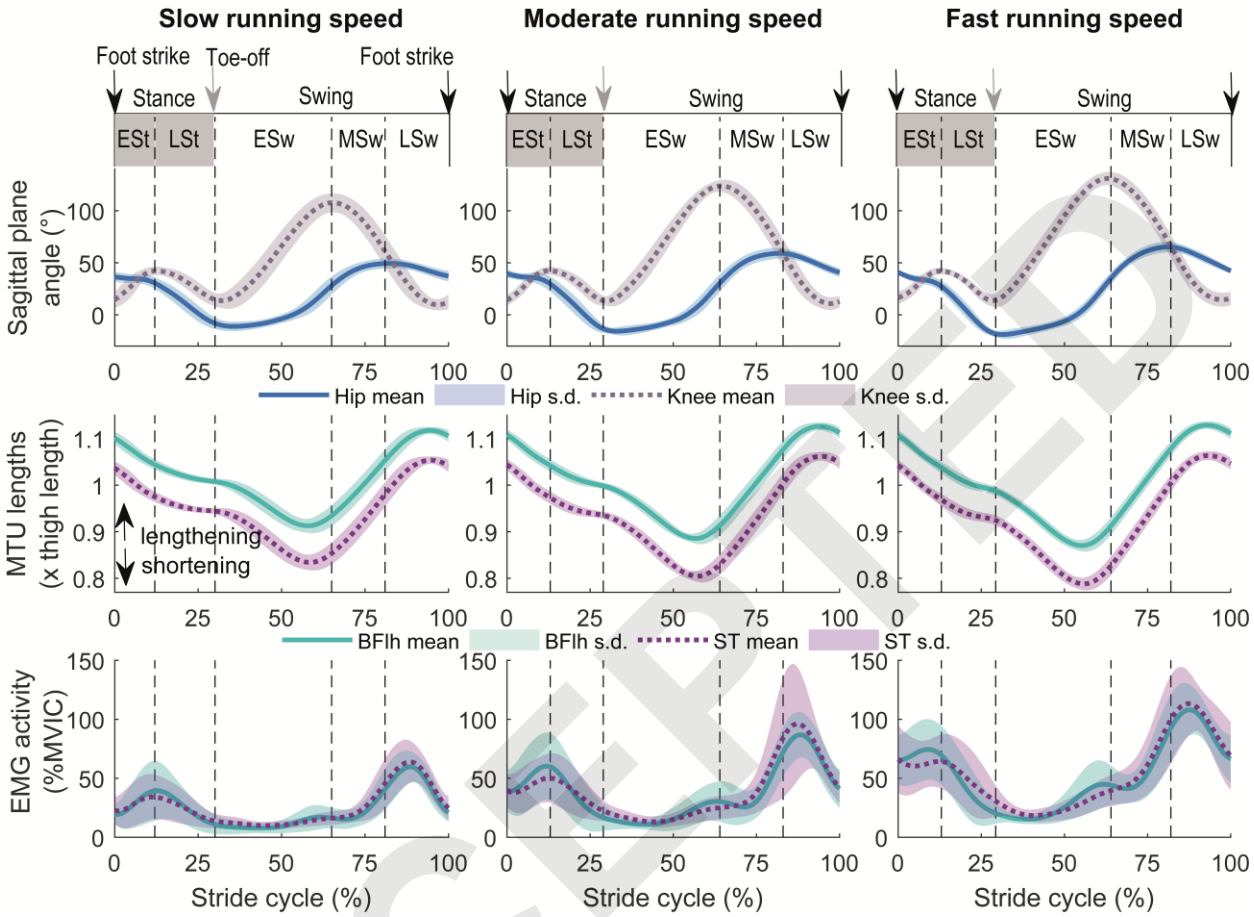

Figure 3

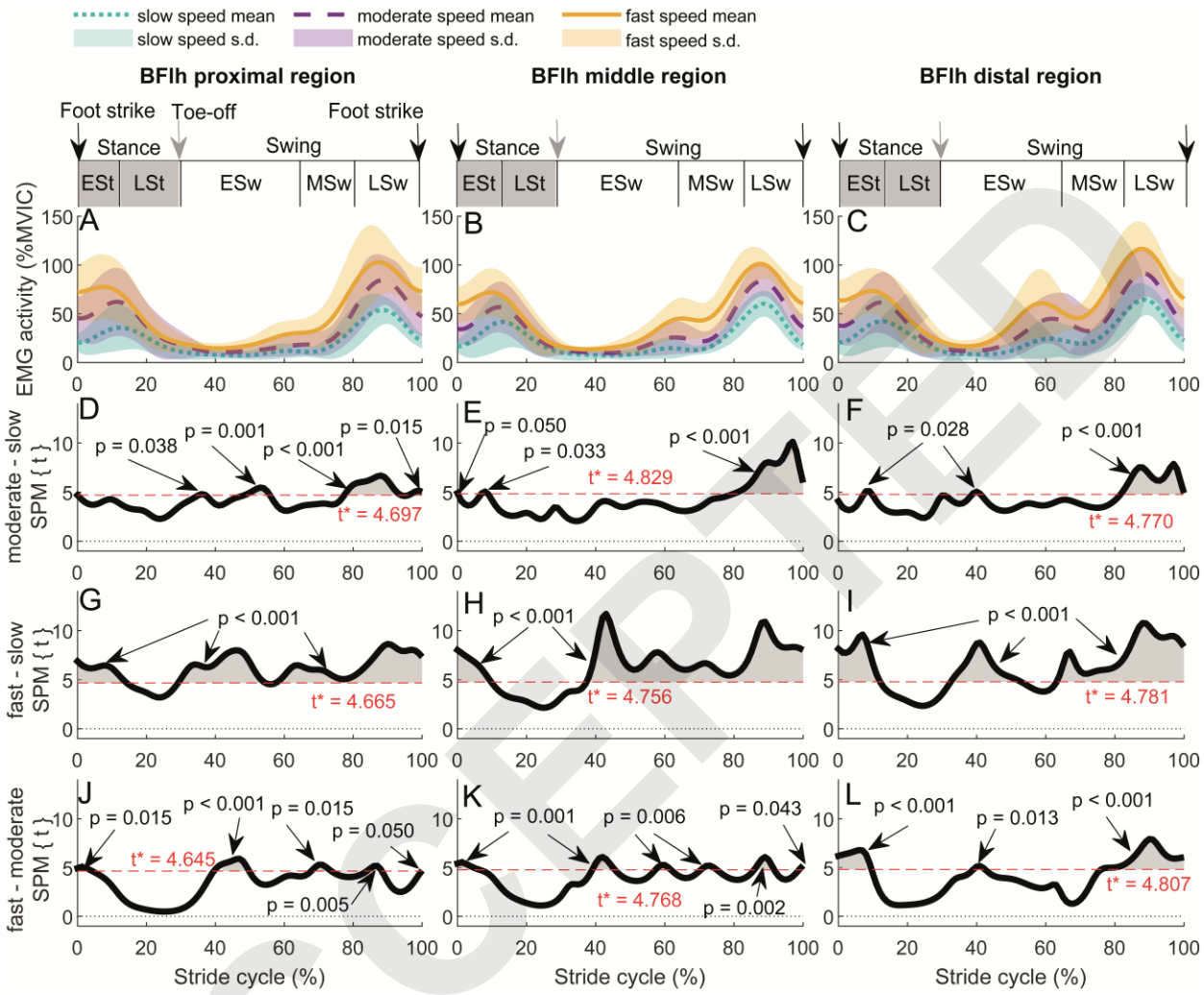

Figure 4

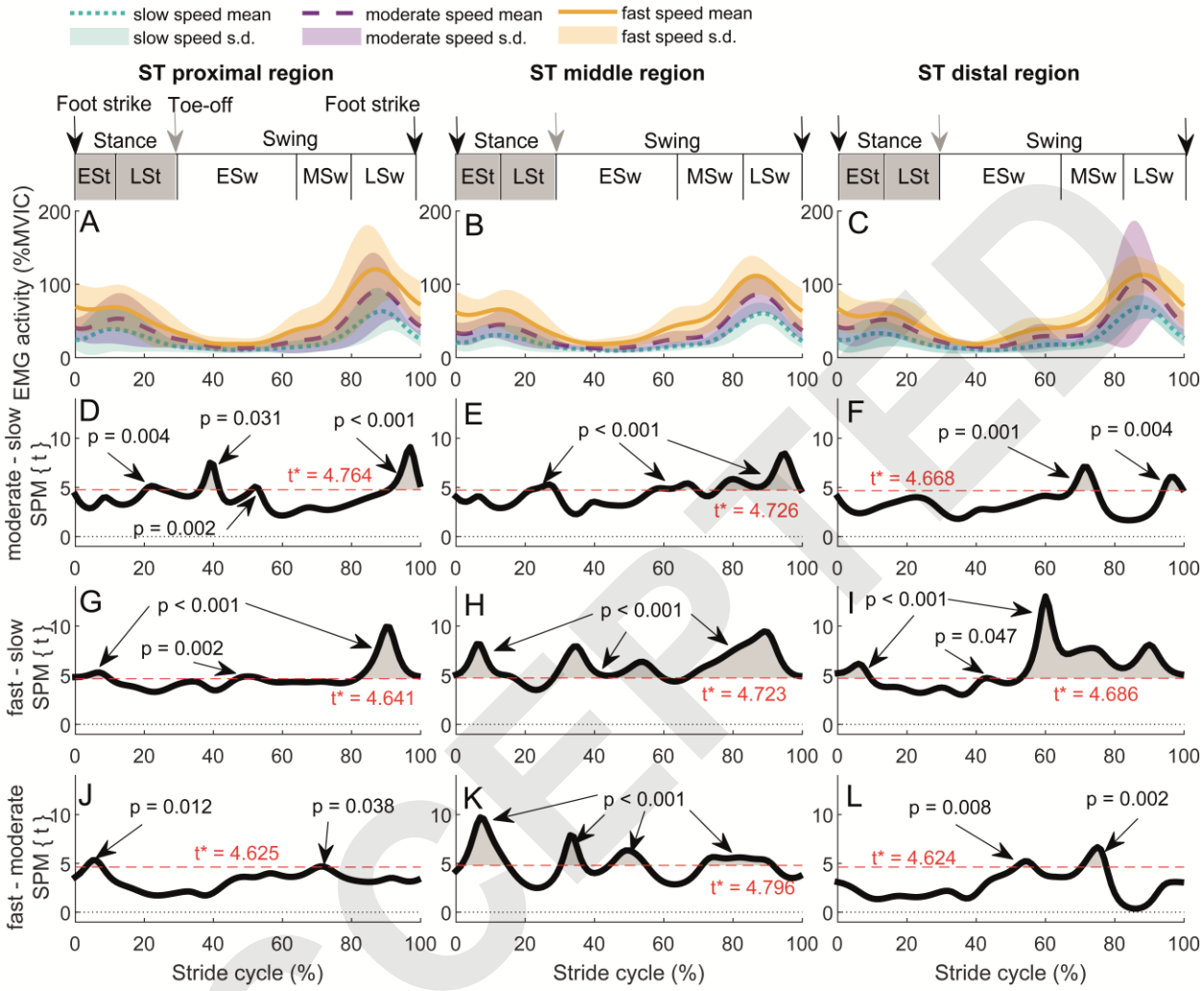

Figure 5

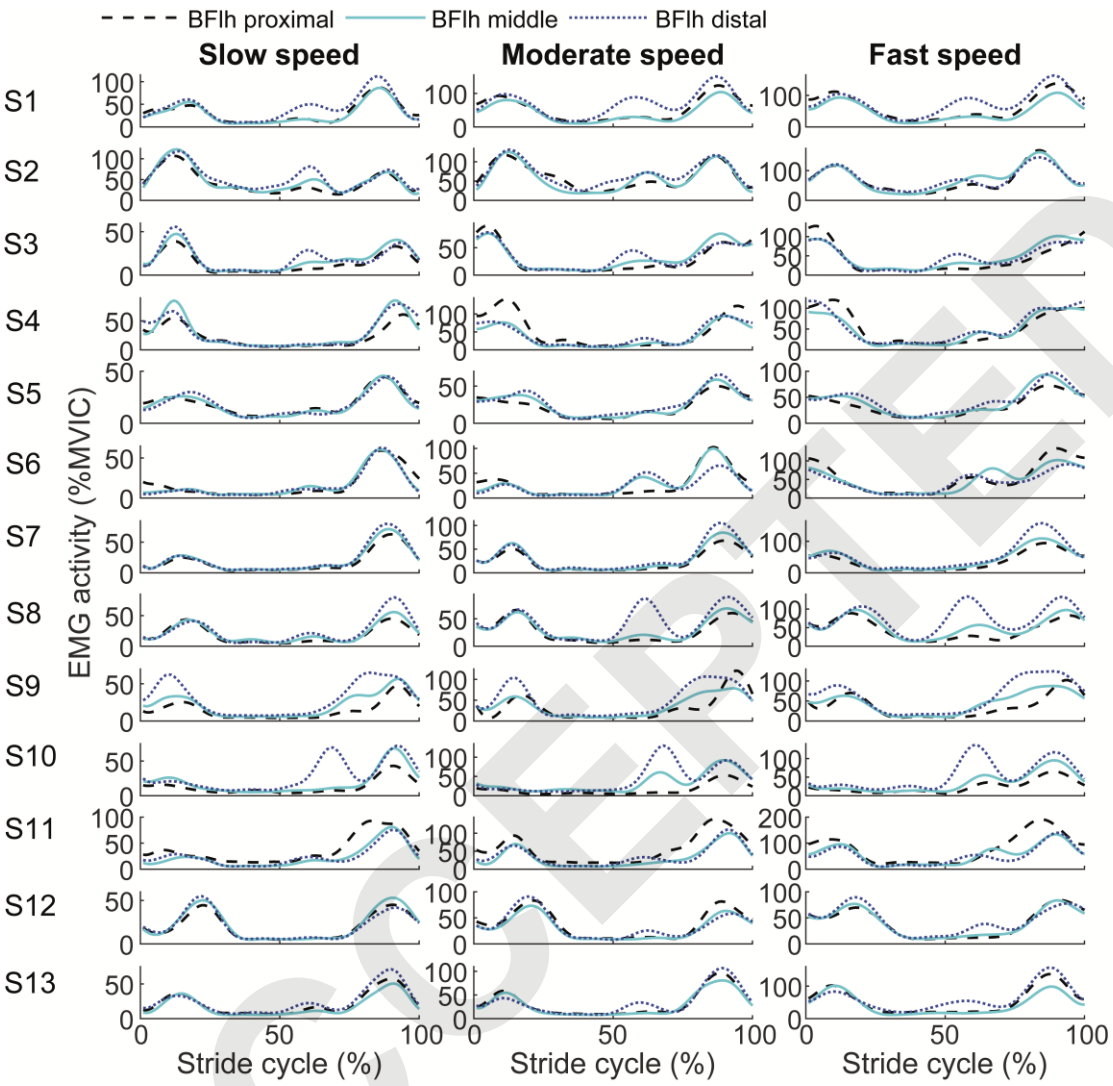

Figure 6

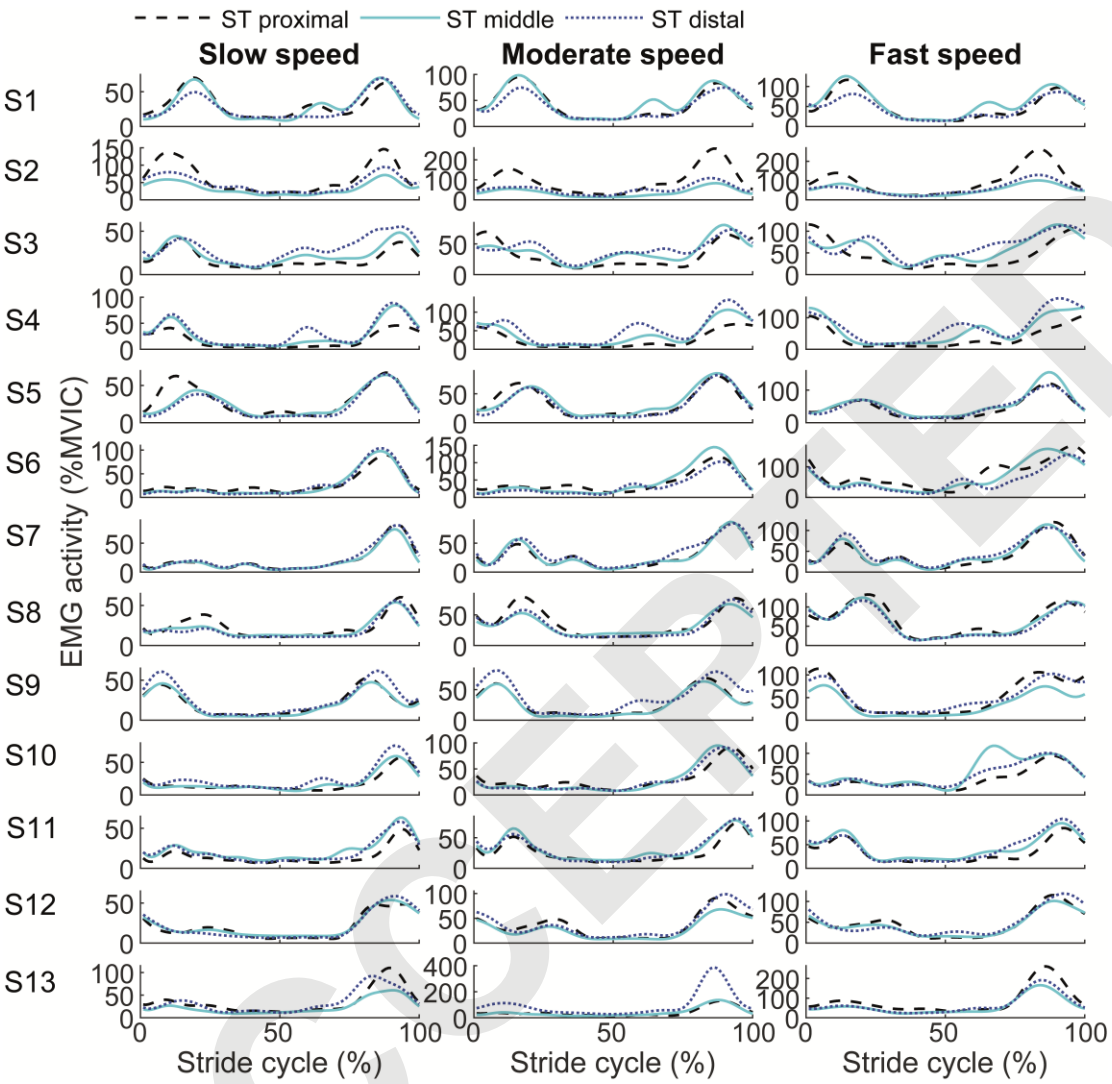

SUPPLEMENTARY FIGURE 1. Upper panels show mean and standard deviation (s.d.) of biceps femoris long head (BFlh) and semitendinosus (ST) electromyography (EMG) activity (normalised to maximal voluntary isometric contraction, MVIC) at slow, moderate and fast running speeds. Lower panels represent corresponding SPM{t} test statistic trajectories (thick black lines). Critical thresholds (t*) are calculated for each comparison after Bonferroni correction (dashed red horizontal lines). These thresholds are not crossed by the SPM{t}, indicating no statistically significant intermuscular differences at any time point of the stride at group level. Running stride sub-phases were defined as early stance (ESt), late stance (LSt), early swing (ESw), mid swing (MSw), and late swing (LSw).

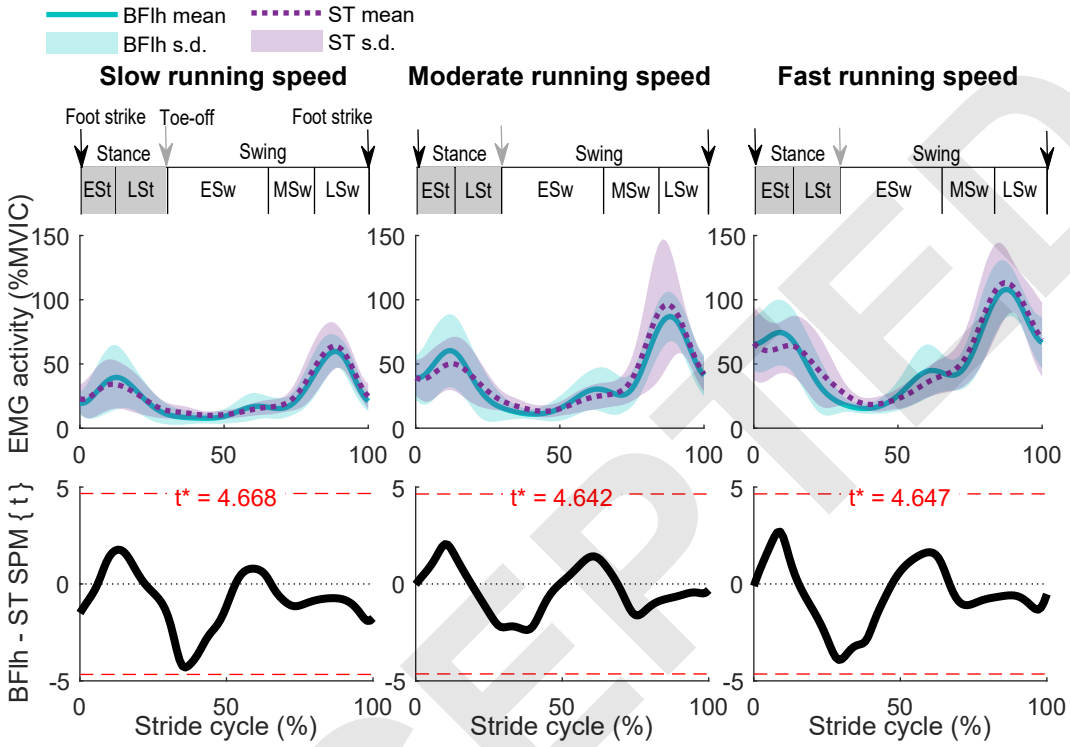

SUPPLEMENTARY FIGURE 2. Effects of running speed on muscle-tendon unit (MTU) lengths. Panels (A) and (B) represent mean and standard deviation (s.d.) across the stride cycle for all running speeds (slow = 4.1 ± 0.2 m·s^{-1}, moderate =5.4 ± 0.3 m·s^{-1}, and fast = 6.8 ± 0.4 m·s^{-1}) for each muscle respectively. Panels (C)-(H) show the statistical parametric maps depicting differences between slow-moderate (C), (D), slow-fast (E), (F), and moderate-fast (G), (H) running speeds in semitendinosus and biceps femoris long head, respectively. Thick black lines represent the SPM{t} test statistics showing the magnitude of the differences relative to s.d. and sample size (N=13). Critical thresholds (t*) are calculated for each comparison after Bonferroni correction (dashed red horizontal lines). Probability (p) values are shown for each supra-threshold cluster depicting statistically significant differences. Running stride sub-phases were defined as early stance (ESt), late stance (LSt), early swing (ESw), mid swing (MSw), and late swing (LSw).

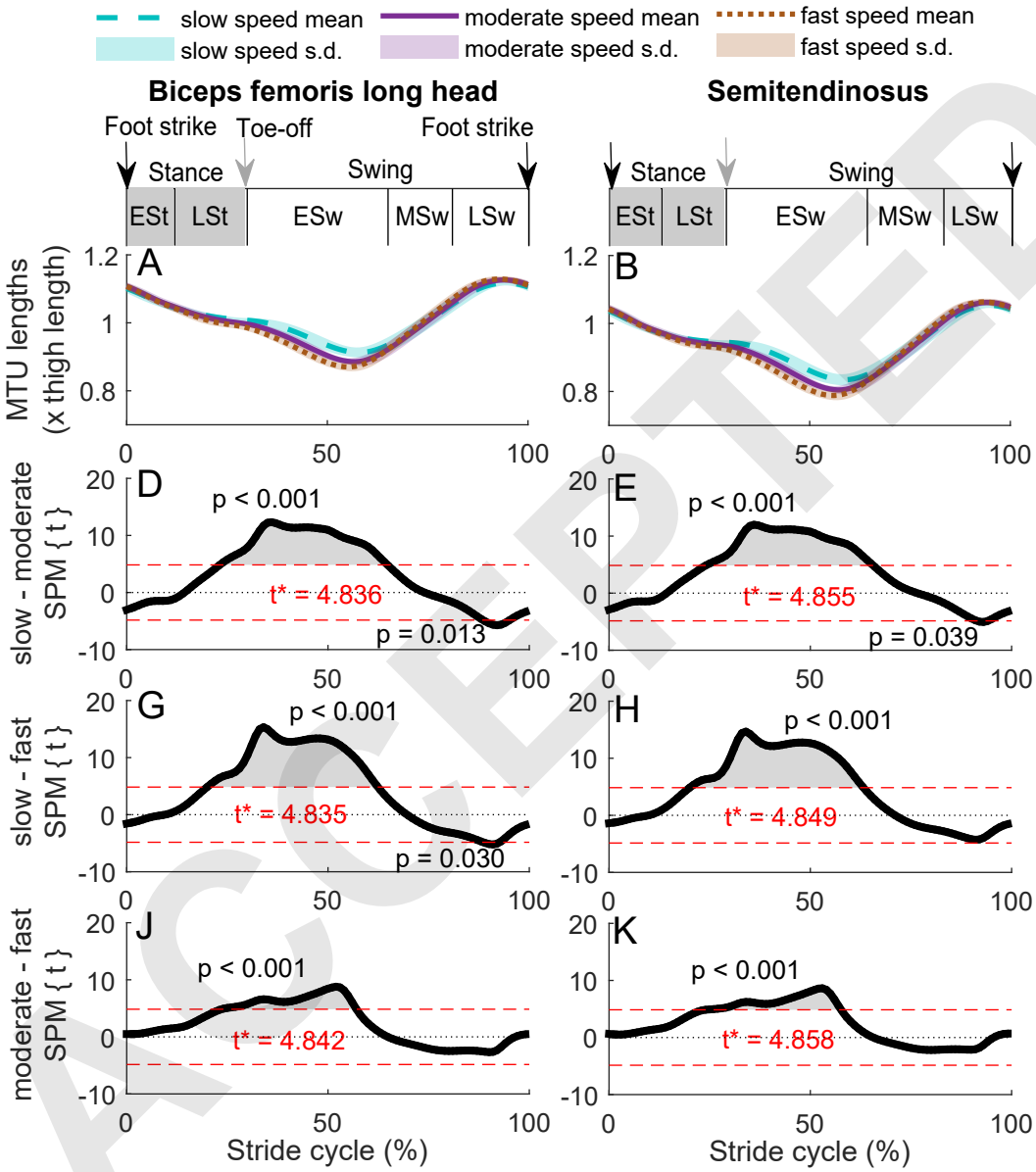

SUPPLEMENTARY FIGURE 3. Similar patterns between individuals S1-S13 in biceps femoris long head (BFlh) and semitendinosus (ST) muscle-tendon unit (MTU) lengths at slow (4.1 ± 0.2 m·s^{-1}), moderate (5.4 ± 0.3 m·s^{-1}), and fast (6.8 ± 0.4 m·s^{-1}) running speeds.

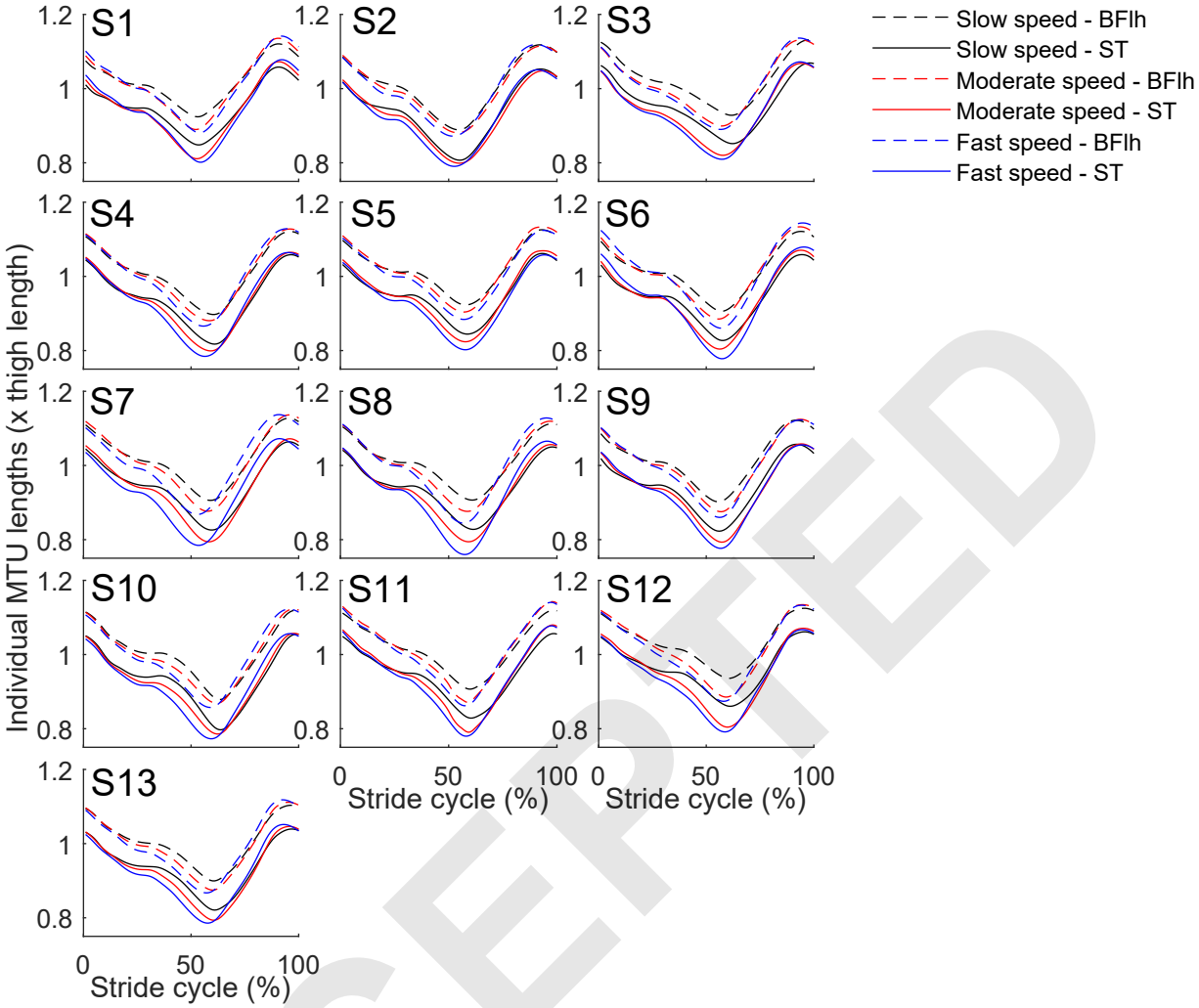

SUPPLEMENTARY FIGURE 4. Inter-individual coefficients of variations in muscle-tendon unit lengths in the early stance (ESt), late stance (LSt), early swing (ESw), mid swing (MSw), and late swing (LSw) at slow (4.1 ± 0.2 m·s^{-1}), moderate (5.4 ± 0.3 m·s^{-1}), and fast (6.8 ± 0.4 m·s^{-1}) running speeds.

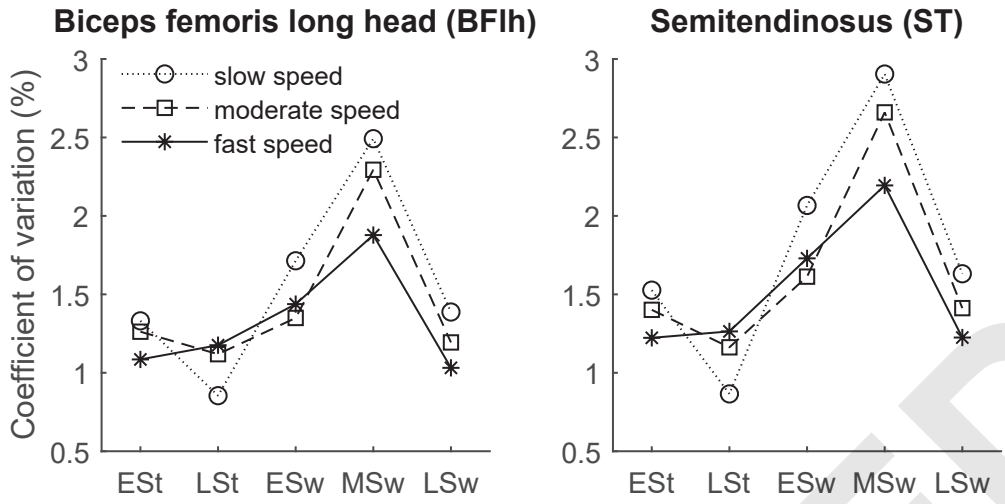

SUPPLEMENTARY FIGURE 5. Regional differences in the electromyography (EMG) activity of biceps femoris long head (BFlh, normalised to maximal voluntary isometric contraction, MVIC). Panels (A)-(C) represent group mean and standard deviation (s.d.) across the stride cycle in each region for each running speed. Panels (D)-(L) show the statistical parametric maps. (D), (E) and(F) show differences between distal and middle regions; (G), (H),and (I) show differences between distal and proximal regions; (J), (K), and (L) show differences between middle and proximal regions at slow (4.1 ± 0.2 m·s^{-1}), moderate (5.4 ± 0.3 m·s^{-1}), and fast (6.8 ± 0.4 m·s^{-1}) running speeds, respectively. Thick black lines are the SPM{t} test statistics representing the magnitude of the differences relative to the s.d. and sample size (N=13).
Critical thresholds (t*) were calculated for each comparison after Bonferroni correction (dashed red horizontal lines; family-wise α = 0.05). SPM{t} trajectory does not cross the t* level in any of the comparisons, indicating no statistical differences between muscle regions. Running stride sub-phases were defined as early stance (ESt), late stance (LSt), early swing (ESw), mid swing (MSw), and late swing (LSw).

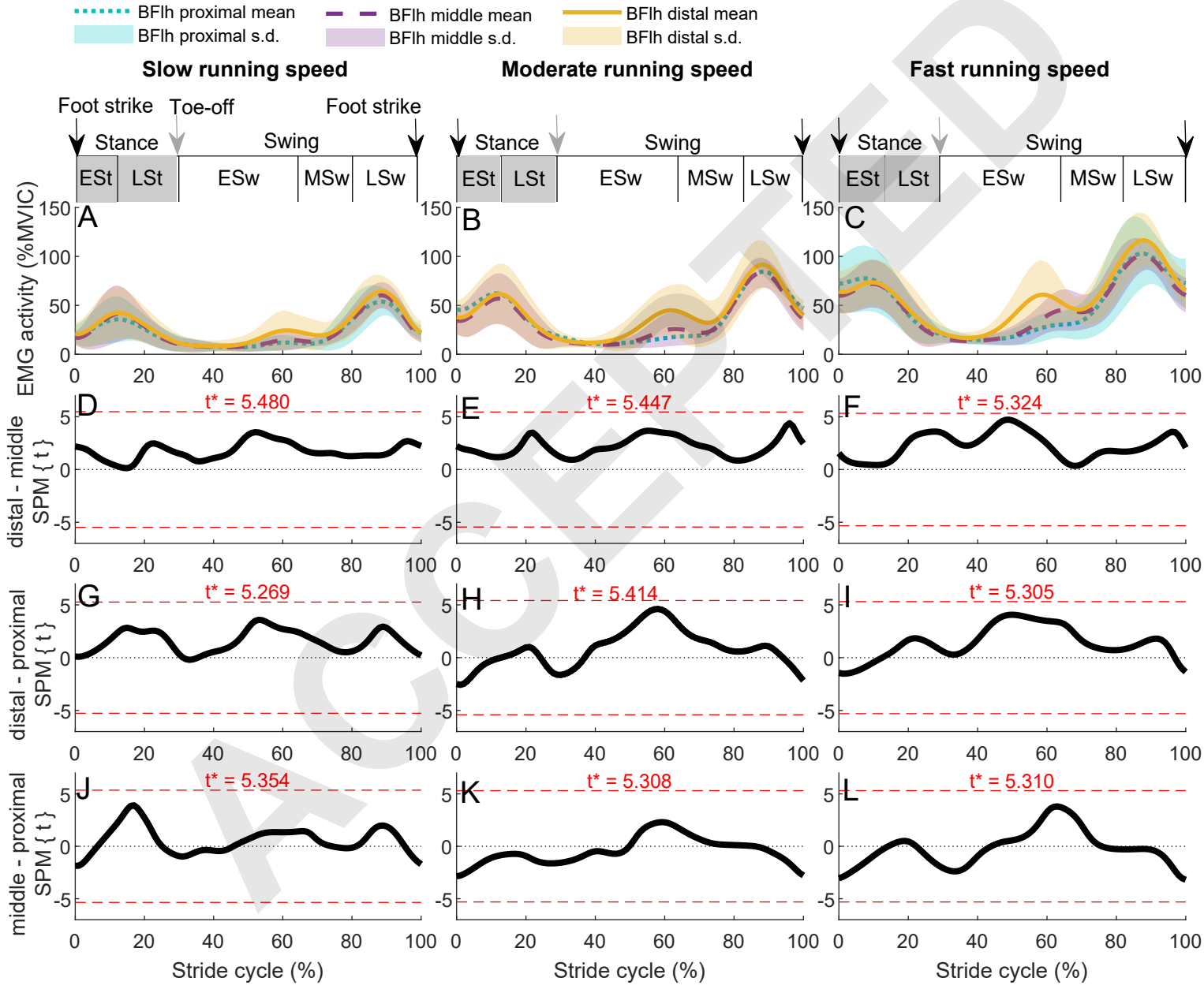

SUPPLEMENTARY FIGURE 6. Regional differences in the electromyography (EMG) activity of semitendinosus (ST, normalised to maximal voluntary isometric contraction, MVIC). Panels (A)-(C) represent group mean and standard deviation (s.d.) across the stride cycle in each region for each running speed. Panels (D)-(L) show the statistical parametric maps. (D), (E) and(F) show differences between distal and middle regions; (G), (H),and (I) show differences between distal and proximal regions; (J), (K), and (L) show differences between middle and proximal regions at slow (4.1 ± 0.2 m·s^{-1}), moderate (5.4 ± 0.3 m·s^{-1}), and fast (6.8 ± 0.4 m·s^{-1}) running speeds, respectively. Thick black lines are the SPM{t} test statistics representing the magnitude of the differences relative to the s.d. and sample size (N=13). Critical thresholds (t*) were calculated for each comparison after Bonferroni correction (dashed red horizontal lines; family-wise α = 0.05). SPM{t} trajectory does not cross the t* level in any of the comparisons, indicating no statistical differences between muscle regions. Running stride sub-phases were defined as early stance (ESt), late stance (LSt), early swing (ESw), mid swing (MSw), and late swing (LSw).

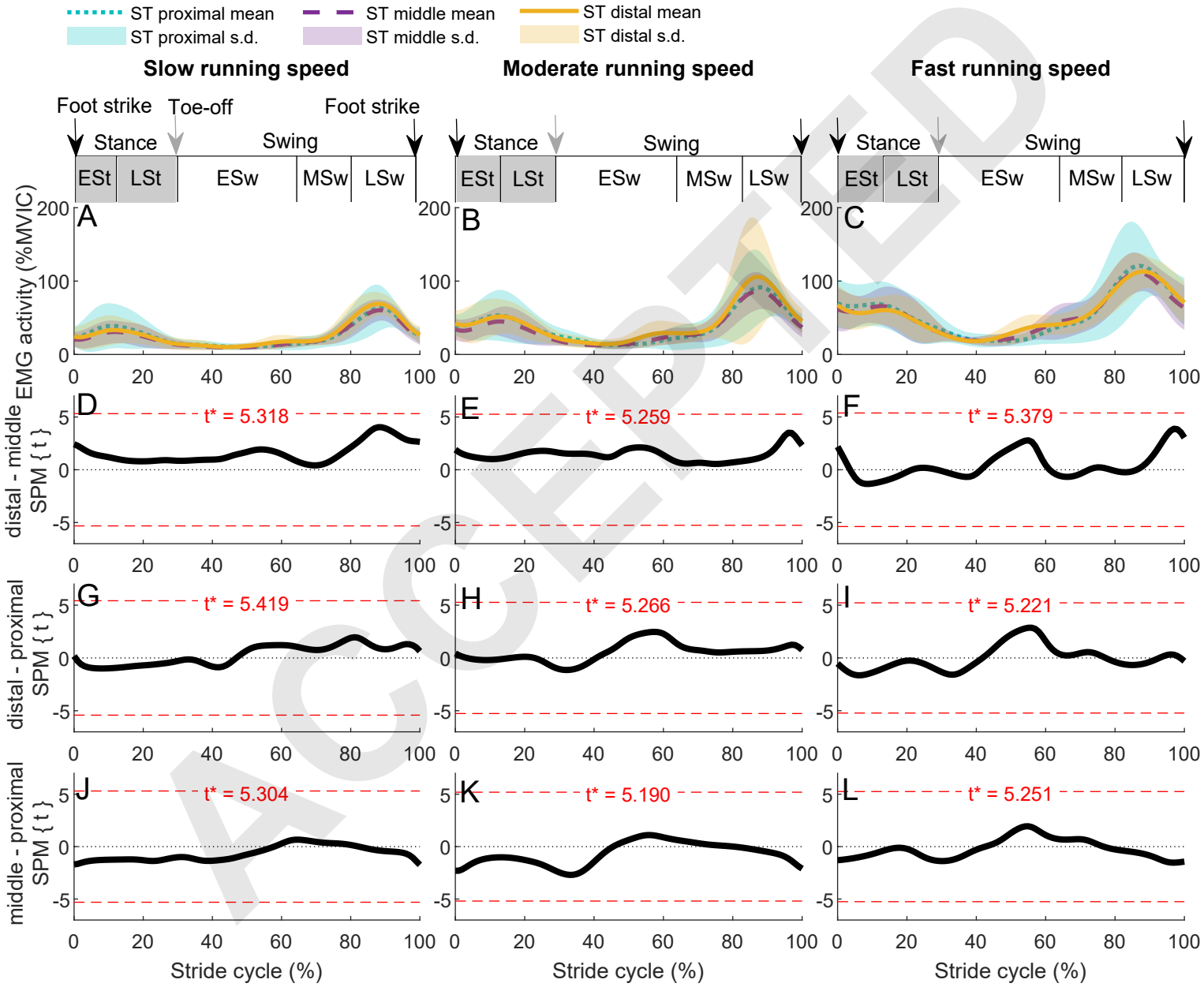

SUPPLEMENTARY FIGURE 7. Large inter-individual coefficients of variations in regional activity levels in the early stance (ESt), late stance (LSt), early swing (ESw), mid swing (MSw), and late swing (LSw) at slow (4.1 ± 0.2 m·s^{-1}), moderate (5.4 ± 0.3 m·s^{-1}), and fast (6.8 ± 0.4 m·s^{-1}) running speeds.

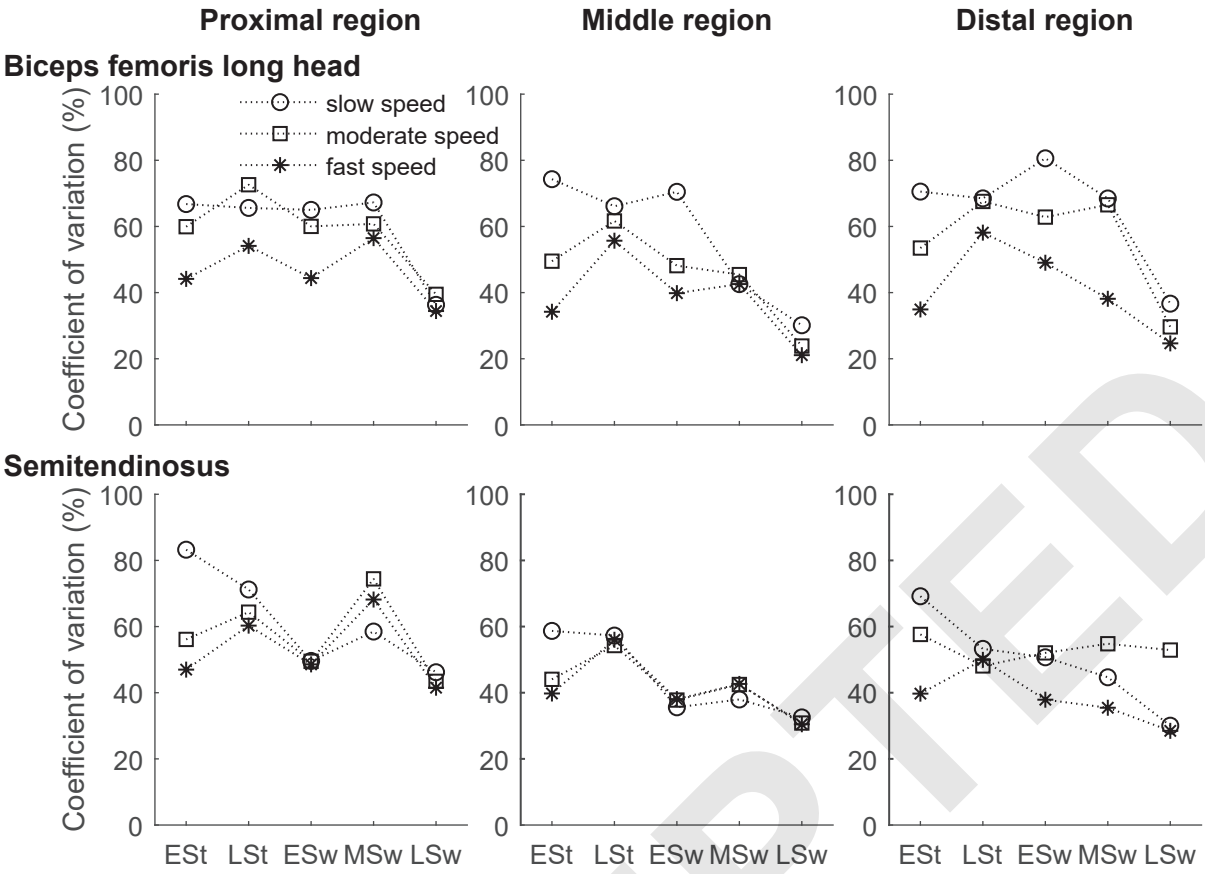

SUPPLEMENTARY FIGURE 8. Individual (S1-S13) muscle-specific electromyography (EMG) activity patterns of biceps femoris long head (BFlh) and semitendinosus (ST) (normalised to maximal voluntary activity, MVIC) at slow (4.1 ± 0.2 m·s^{-1}), moderate (5.4 ± 0.3 m·s^{-1}), and fast (6.8 ± 0.4 m·s^{-1}) running speeds when all EMG channels are averaged along each muscle. Note that scaling of the y axis is optimised for each individual so that intermuscular differences are easier to identify. Foot strike is at 0% and 100% of the stride.

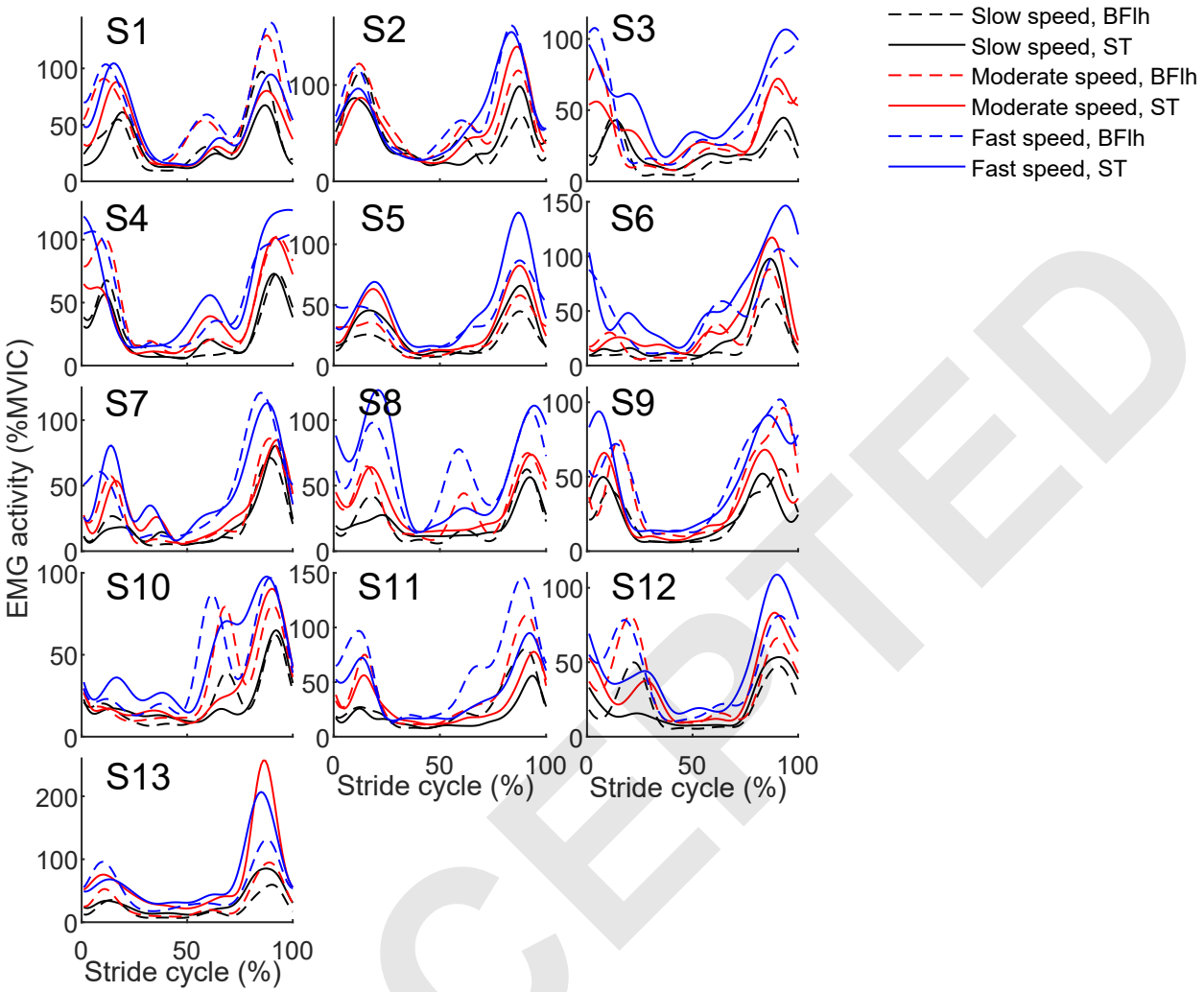

SUPPLEMENTARY FIGURE 9. Large inter-individual coefficients of variations in muscle activity levels at slow (4.1 ± 0.2 m·s^{-1}), moderate (5.4 ± 0.3 m·s^{-1}), and fast (6.8 ± 0.4 m·s^{-1}) running speeds when all (up to 15) electromyography (EMG) channels are averaged along each muscle. Sub-phases of the running stride: early stance (ESt), late stance (LSt), early swing (ESw), mid swing (MSw), and late swing (LSw).